Chemical Geology 367 (2014) 39–50

Contents lists available at ScienceDirect

Chemical Geology

journal homepage: www.elsevier.com/locate/chemgeo

Reactive transport modelling of geologic CO_2 sequestration in saline aquifers: The influence of pure CO_2 and of mixtures of CO_2 with CH_4 on the sealing capacity of cap rock at 37 °C and 100 bar

S. Mohd Amin [a,b,*], D.J. Weiss [a,c,d], M.J. Blunt [a]

[a] Department of Earth Science and Engineering, Imperial College London, London SW7 2AZ, United Kingdom
[b] Civil Engineering Department, University of Malaya, 60503 Kuala Lumpur, Malaysia
[c] Mineralogy, The Natural History Museum London, London SW7 5PD, United Kingdom
[d] Stanford University, 450 Serra Mall, CA 94305, United States

ARTICLE INFO

Article history:
Received 11 July 2013
Received in revised form 3 January 2014
Accepted 3 January 2014
Available online 13 January 2014

Editor: J. Fein

Keywords:
Reactive transport model
CO_2 storage
Impurities
Porosity
Cap rock

ABSTRACT

The costs of CO_2 separation for carbon capture and storage can be reduced through capturing less pure CO_2. The presence of impurities such as methane (CH_4) in the CO_2 gas stream, however, affects the geochemical and geophysical processes in the subsurface. The dissolved CO_2 in the brine decreases the pH which dissolves minerals such as calcite and albite. The dissolution of these minerals increases the amount of Ca^{2+} and Na^{+} in the brine. The presence of these ions leads the precipitation of the secondary solid carbonates calcite and dawsonite. To test this process, we developed a kinetic batch and a one-dimensional reactive transport model using PHREEQC 2.15.0, to predict mineral alteration induced in the cap rock by penetration of brine containing dissolved CO_2 from the underlying aquifer over a period of 10,000 years. The chemical composition of the Nordland shale formation water that overlies the Utsira sand in the Sleipner field was used as a model case in this study. The model was run for pure CO_2 and for mixtures with CH_4 (1–4 (w/w)%) in the injected gas stream at a temperature of 37 °C and at a pressure of 100 bar. The simulations suggest that a mixture of CO_2 and CH_4 suppresses an anticipated increase in the porosity of the cap rock. Thus, our results suggest that injection of a CO_2–CH_4 mixture inhibits cap rock dissolution and helps maintain the sealing capacity of the cap rock, while reducing separation costs.

1. Introduction

Carbon dioxide (CO_2) is usually injected during carbon storage into geological reservoirs at temperatures and pressures above critical values, i.e., $T_c = 31.1$ °C and $p_c = 7.38$ MPa. Under these conditions, the CO_2 is present as a dense phase although it is lighter than the formation brine. Consequently, the injected CO_2 rises buoyantly to the top of the aquifer formation and accumulates underneath the cap rock (Lindeberg and Wessel-Berg, 1997). Oilfield and saline aquifers that rely on structural trapping for CO_2 storage include Weyburn in Saskatchewan, Canada (Malik and Islam, 2000) and Sleipner in the North Sea, Norway (KØrbol and Kaddour, 1995), respectively.

Cap rocks are low porosity and low permeability seals saturated with brine through which other fluids either cannot flow or only flow extremely slowly. In particular, the seal has a high capillary entry pressure that acts to stop the entry of supercritical CO_2. Common seal lithologies are salts, anhydrites, and silty or clay mineral-rich shales. Leakage through cap rocks can occur in three ways: (i) rapid ("catastrophic") by seal-breaching (mechanical failure) or damage of the well casing (i.e., corrosion of pipes and cements); (ii) long-term, controlled by the capillary sealing efficiency (essentially the cap rock is eroded and becomes more porous and permeable); and (iii) diffusive loss of dissolved CO_2 through the water-saturated pore space.

CO_2 transport through cap rocks occurs by molecular transport (diffusion) through the water-saturated pore system since Darcy flow rates are negligible. This process is considered of little relevance in terms of CO_2 loss (Busch et al., 2008), but it can control the rate of geochemical reactions taking place in the cap rock, i.e., the dissolved CO_2 can allow dissolution of the cap rock. As a result, this affects rock properties such as porosity, permeability and tortuosity, hence admitting flow and allowing CO_2 to escape to the surface. Only a few experimental and numerical results on molecular diffusion of CO_2 through cap rock have been published (Angeli et al., 2009). However, the characterization of cap rock alteration caused by molecular diffusion on chemical reactions and dissolution/precipitation of minerals, especially for long term containment, is of great importance for the design of safe storage.

* Corresponding author at: Department of Earth Science and Engineering, Imperial College London, London SW7 2AZ, United Kingdom. Tel.: +44 60379675153.
E-mail address: smohdami@imperial.ac.uk (S. Mohd Amin).

0009-2541/$ – see front matter © 2014 Elsevier B.V. All rights reserved.
http://dx.doi.org/10.1016/j.chemgeo.2014.01.002

Dissolution of CO_2 into the cap rock brine can form acidic solutions that lead to the dissolution of minerals such as calcite and dawsonite. These minerals can precipitate later given the right conditions and consequently store CO_2 in a stable solid phase with increasing storage security. The formation conditions for calcite and dawsonite depend on availability of metal cations such as Ca^{2+} and Na^{+} (Hellevang et al., 2005). These minerals react at moderate to high CO_2 partial pressures and in highly alkaline solutions (Smith and Milton, 1966; Baker et al., 1995; Hellevang et al., 2005; Moore et al., 2005; Golab et al., 2006; Worden, 2006; Gao et al., 2009).

Previous laboratory experiments and modelling studies have been conducted to assess the potential of mineral trapping in cap rock for a wide range of different geological systems (Czernichowski-Lauriol et al., 1996; Gunter et al., 1997; Rochelle et al., 2002; SACS2, 2002; Kaszuba et al., 2003; Johnson et al., 2004; Gaus et al., 2005; Bertier et al., 2006; Gherardi et al., 2007; Wigand et al., 2008). These studies showed that mineral alterations, such as dissolution of calcite, are caused by the formation of bicarbonate with a decrease in pH during CO_2 injection. Some studies have addressed the impact of these changes on the porosity in cap rocks (Busch et al., 2008; Hangx et al., 2009). All of these studies show good sealing capacity through precipitation of minerals. Important insights on cap rock mineralogical alteration patterns induced by CO_2 migration have been gained by means of reactive transport modelling (Johnson et al., 2004; Gaus et al., 2005; Johnson and Morris, 2005; Xu et al., 2005; Gherardi et al., 2007). None of these studies, however, have assessed the impact of impurities such as methane (CH_4) on the CO_2 on sealing capacity.

Depending on the industrial source (energy production, natural gas processing, iron industry, concrete production) and capture processes, the composition of the gaseous CO_2-rich mixture emitted varies considerably in chemical composition and concentration. The degree of purity of the captured CO_2 is a key factor for injection and sequestration. In addition to CO_2 and traces of water, other gases, such as CH_4 may be present in the mixture. The most common current application of CO_2 capture and storage is for CO_2 removal from natural gas such as at Sleipner field in the North Sea (Baklid et al., 1996). At this site, CO_2 is removed from natural gas with methyldiethanolamine, compressed and transported in a pipeline for injection via a well. The most common impurity in the CO_2 is CH_4 (Austegard et al., 2006). It has been suggested that CH_4 with a concentration in the range 1–4 (w/w%) could be injected with the CO_2 (De Visse et al., 2008). The admixing of CH_4 affects the compressibility of the injected CO_2 and reduces the storage capacity of the free phase. In addition, CH_4 impurities affect the aqueous solubility and the rates of mineral dissolution and precipitation (KØenen et al., 2011).

The aim of this paper is to study the geochemical aspects of long-term integrity of the cap rock and of possible upward migration after injection of CO_2 with and without methane impurities. Special attention is placed on the mineral dissolution/precipitation of two important carbonates: calcite and dawsonite. In addition, changes in porosity from dissolution/precipitation of these minerals are investigated. To achieve this, reactive transport modelling combining reaction kinetics and diffusive transport in alumina silicate-rich shales was performed. The model site investigated is the Sleipner field, where CO_2 has been successfully injected and stored since 1996 (KØrbol and Kaddour, 1995). Published, site-specific geochemical data from the Nordland shale that overlies the Sleipner field is used to describe the cap rock. Gas–water–rock interactions resulting from CO_2 migration into the cap rock are simulated assuming diffusive transport. Simulations are run using pure CO_2 and variable mixtures of CO_2 with CH_4 (1–4 (w/w)%). Fluid–rock interactions in sealed cap rock have been modelled using a kinetic batch and one-dimensional molecular-diffusion kinetically controlled model at a temperature of 37 °C and a pressure of 100 bar employing the PHREEQC 2.15.0 code (Parkhurst and Appelo, 1999). The change in porosity is calculated from changes in solid volume. The simulations were run for 10,000 years, which is the relevant timescale for the long-term safety assessment of CO_2 storage (Bowden, 2005; Credoz et al., 2009).

2. Materials and methods

2.1. Geochemical data

We modelled our system using as input data the initial formation water composition and the primary cap rock mineral assemblage of the Sleipner site (Czernichowski-Lauriol et al., 2002; Johnson et al., 2004). Literature data was used for molar volumes, reaction rate parameters and specific surface areas for the primary and secondary minerals albite, chalcedony (quartz), dawsonite, illite, k-feldspar, siderite, magnesite, calcite, clinochlore-7A, dolomite-dis, kaolinite, pyrite, and smectite-high-Fe-Mg (see references in Table 2). The mineral assemblages are taken from samples collected from the Nordland shale. This shale is a well-characterized cap rock that is effectively impermeable to CO_2 and acts as important barrier of buoyant CO_2 leakage to the surface.

2.2. Cap rock formation water

The chemical composition of the formation water in the Nordland shale is unknown. We represent the formation water using a pore water sample from the Oseberg field, which is located 200 km north of Sleipner. We equilibrated the formation water with the mineralogy of the Nordland shale and the resulting composition (Table 1) wasused as the starting point for subsequent modelling in this study (Czernichowski-Lauriol et al., 2002). A total of 11 aqueous components (Table 1) were included in the simulations.

2.3. Kinetic parameters

The dissolution and precipitation of minerals in the system was kinetically controlled during the batch and molecular diffusion modelling. The reaction rates were derived from previous work following the relevant formulae (Lasaga, 1984):

$$rate_m = A_m k(T)_m (a_{H^+})^n [1\text{-}(Q_m/K_m)] \quad (1)$$

where the subscript m is the mineral index, $rate_m$ is the dissolution/precipitation rate (positive values indicate dissolution, negative values precipitation), A is the reactive surface per kg water, $k(T)$ is the temperature dependent rate constant, a_H is the proton activity, n is the order of reaction ($0 \le n \le 1$), K_m is the equilibrium constant for the mineral water reaction written for the dissolution of 1 mol of mineral, and Q_m is the reaction quotient. We assumed for all minerals that the precipitation rate equals the dissolution rate and that the secondary minerals (dawsonite, magnesite, etc) precipitate following the dissolution of the albite and calcite. This is a simplified assumption; however, in absence of accurate data of precipitation and dissolution rates under

Table 1
Initial fluid composition of the formation water in the cap rock from equilibration of the Nordland shale mineralogy with the formation water from the Utsira sand.
Taken from Czernichowski-Lauriol et al. (2002).

Parameter	Value	Elements	Concentration (M)
Temperature (°C)	37	Al	3.51×10^{-8}
Ionic strength	0.647	Ba	1.25×10^{-5}
pH	7.67	C	6.92×10^{-5}
pe	−4.07	Ca	1.77×10^{-1}
		Cl	4.79×10^{-1}
		Fe	2.48×10^{-7}
		K	1.42×10^{-4}
		Mg	1.11×10^{-2}
		Na	1.06×10^{-1}
		S	4.81×10^{-4}
		Si	2.52×10^{-4}

Note: pe is used to indicate the redox conditions of the system. Positive values of pe indicate oxidising conditions and negative values indicate reducing conditions.

field conditions, this approximation is justified. Rate laws determined in the laboratory can differ from field rates by orders of magnitude (Appelo and Postma, 2005).

The rate constants for all minerals were extrapolated to field conditions – a temperature of 310.15 K – from reported rate constants at 298.15 K using the Arrhenius relation (Table 1):

$$k = k_{25}[-E_a/R(1/T-1/298.15)] \quad (2)$$

where E_a is the activation energy (J/mol), k_{25} is the rate constant at 298.15 K (mol/m^{2}s), R is the gas constant (8.314 J/mol K) and T is the temperature (K). The rate constants at 298.15 K are taken from the literature (Table 1).

The kinetic rate law used for pyrite was different (Wiersma and Rimstidt, 1984):

$$rate_{pyrite} = k(T)A\left(Fe^{3+}\right)/m_{solution} \quad (3)$$

where $m_{solution}$ is the mass of the solution (kg), A is the reactive surface area of pyrite, and Fe^{3+} is the concentration (mol/l). This rate law best represents the contribution of Fe^{3+} to the oxidation of pyrite (Stumm and Morgan, 1996).

The parameters to calculate kinetic rates of minerals are given in Table 2. The dissolution and precipitation of all minerals are kinetically controlled. Rate law constants for minerals were taken from various sources in the literature and are summarized in Table 2. We note that literature data for the value of the power (n) in the rate expression of Eq. (1) are fragmentary and often inconsistent. Thus, we used an uniform value of 0.5 for all minerals in agreement with previous studies (Gaus et al., 2005).

The reactive surface area of the rock was represented by spherical grains with two grain diameters: 2×10^{-6} m for the clay minerals; and 3.3×10^{-5} m for the non-clay minerals. Reactions between minerals and fluid are expected to take place at the reactive surface area. Differences between total and reactive surface area can differ by up to three orders of magnitude explaining the discrepancy between laboratory measured and field rates (Appelo and Postma, 2005). The difference is because often large parts of the mineral surface involved in the reactions are covered by coatings (other minerals, biofilms etc) with only a small fraction of clean surface exposed to the brine. To account for this, a scaling factor of 0.001 was applied to all minerals. This also defines the ratio of the BET to geometric surface area. This approach has been successfully used before (Zerai et al., 2006). Table 2 shows the specific surface areas for all minerals. The calculated surface areas (Gaus et al., 2005) are shown in Table 2. For Nordland shale, no direct BET measurements are available to help refine these estimates. The larger surface areas for clay minerals (kaolinite, smectite-high-Fe-Mg, and illite) are due to smaller grain sizes.

2.4. Modelling approach

2.4.1. Conceptual model and simulation conditions

The fluid–rock interactions of a homogenous cap rock have been tested using two sets of simulations: kinetic batch and molecular diffusion modelling. The kinetic batch modelling assesses the rate of reaction, assuming that CO_2, brine and the rock are always in mutual contact. The diffusion modelling assesses how dissolved CO_2 may penetrate the cap rock, causing dissolution or precipitation in a transient front that moves, slowly, through the formation.

In the kinetic batch model, we started with 150 l of brine, an initial porosity of 0.15, and the total volume of the porous medium is 1 m^3, including the rock. The geochemical reactions are not limited by the availability of solid minerals, and are therefore insensitive to the rock volume (Fig. 1). We started from a chemically, hydrologically and geometrically simplified batch system at chemical equilibrium. This was done in the absence of CO_2; the initial brine composition in the cap rock is given Table 1 with the minerals listed in Table 2, and was run for 20 years: this established the initial conditions for the simulations to follow.

Subsequently, we added an initial amount of either 150 kg pure CO_2 or 150 kg of a mixture of CO_2 with CH_4 (1–4 w/w%) with the cap rock and 150 l of brine. At this stage, the simulations were run using different kinetic parameters for a period of 10,000 years. This time period was chosen as this is the legal minimum retention time to contain CO_2 safely in saline aquifers (Lindeberg, 2002). Simulations were performed at isothermal conditions of 37 °C. At a depth of 800 m, the pressure of the Utsira formation is assumed to be 100 bar. These values mean that the CO_2 is under supercritical (sc) conditions. Under these pressure and temperature conditions, the fugacity coefficients were computed for CO_2 (sc) and CH_4 (sc) species using the virial equation given elsewhere (Duan et al., 1992).

For the simulations including molecular diffusion with a spatial evolution of a reacting front, the model was run with no net flow of brine in a one-dimensional model consisting of a 10 m column of cap rock (Fig. 2). The computational domain was divided into 10 cells; each one is a 1 m^3 cube. Each cell is denoted as a Representative Elementary Volume (REV) with an initial porosity of 0.15 which contains 150 l of brine; again we assume that the reactions are not limited by the availability of solid minerals. The simulations were performed at isothermal conditions of 37 °C. The initial composition of the cap rock brine is given in Table 1. The lower end of the domain was in contact with the permeable aquifer, where we maintain a brine composition that is fully saturated with CO_2 (or the CO_2–CH_4 mixture). We assume that the

Table 2
Kinetic rate parameters for the primary and secondary minerals of Nordland shale. Taken from BØe and Zweigel (2001).

Minerals	Amount present/mol per REV	Molar volume/ 10^{-6} m^3/mol	Specific surface area/$\times 10^{-2}$ m^2/g	Rate constant/mol/m^2 s	Source of kinetic rate constant
Albite	25.6	100.25	6.95	−8.44	Blum and Stillings (1995)
Calcite	5.6	36.93	6.71	−6.35	Lee and Morse (1999)
Chalcedony (Quartz)	196.0	22.69	6.86	−11.73	Rimstidt and Barnes (1981)
Clinochlore-7A	4.0	20.98	11.3	−11.63	Nagy (1995)
Dawsonite	0	59.30	8.49	−6.86	Intermediate calcite/dolomite
Dolomite-dis	0	64.39	6.35	−7.38	Pokrovsky and Schott (2001)[a]
Illite	35.21	59.89	46.8	−13.08	Set to muscovite rate
Kaolinite	38.15	99.52	116.0	−12.54	Nagy (1995)
K-feldspar	4.08	108.87	7.11	−8.79	Blum and Stillings (1995)
Pyrite	12.90	23.94	3.63	−3.72	Wiersma and Rimstidt (1984)
Siderite	8.60	29.37	4.61	−7.38	As dolomite
Smectite-high-Fe–Mg	11.93	140.71	104	−13.25	Set to muscovite rate (Nagy, 1995)
Magnesite	0	28.02	6.04	−7.38	As dolomite

[a] Average value from these authors.

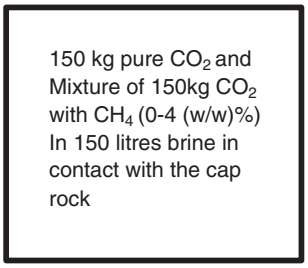

Fig. 1. Conceptual diagram of the kinetic batch model. The model contains rock with a porosity of 0.15 in contact with 150 l of brine. This cap rock is equilibrated with 150 kg of pure CO_2 or of a mixture of CO_2 with CH_4 (0–4 (w/w)%).

supercritical CO_2 is trapped in the aquifer and the acidic brine ingresses into the cap rock by diffusion of dissolved species only. The diffusion coefficients for all aqueous species in the cap rock and aquifer listed in Tables 1 and 3 are calculated and discussed in Section 2.4.3. The chemical and mineral composition of the cap rock is given in Tables 1 and 2. As in the kinetic batch modelling, it was assumed that the aquifer was situated at a depth of 800 m where the pressure of the Utsira formation was assumed to be 100 bar.

2.4.2. Modelling code

All simulations were performed for 10,000 years using the computer code PHREEQC 2.15.0. This code is based on an ion-association aqueous model that simulates kinetically controlled batch reactions.

The Debye–Hückel equation was used to calculate the activity coefficients of the species. The Pitzer equations are arguably better suited to high ionic strength solutions such as the brines tested in this model (Gaus, 2010); however, in the PHREEQC code, the distribution of species including SiO_2 and Al^{3+} in solution is not taken into account and only free ions are recognized. These assumptions preclude the use of minerals such as albite, quartz, and feldspar in the model. Using the Debye Hückel model likely overestimates the activity coefficients for all of the aqueous species.

The code is supplemented with a number of thermodynamic databases that provide equilibrium constants (Parkhurst and Appelo, 1999). The Vantt' Hoff equation was used to adjust the reaction enthalpies to temperature changes and the equilibrium constants. The

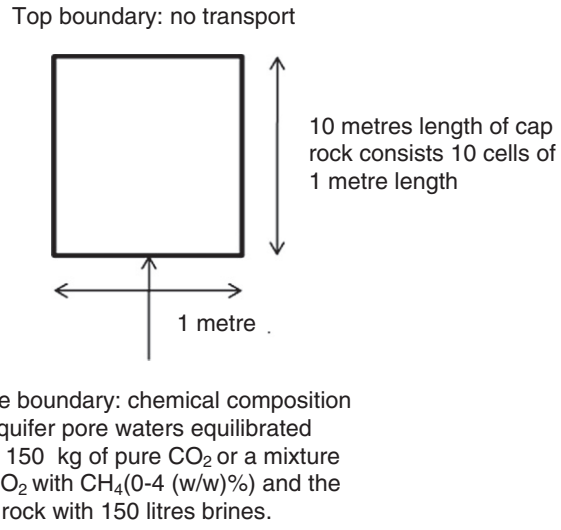

Fig. 2. Conceptual diagram of the one-dimensional reactive transport model. Each cell has a volume of 1 m^3 of Nordland shale with an initial porosity of 0.15 and, 150 l of brine. Lower boundary conditions: the aquifer brine at the base of the system in contact with the permeable aquifer is assumed to be fully saturated with 150 kg of pure CO_2 or a mixture of CO_2 with CH_4 (0–4 (w/w)%). Top boundary conditions: no transport. The effective diffusion coefficient for all aqueous species listed in Tables 1 and 2 is 3.33×10^{-10} m^2/s.

Table 3
Initial fluid composition of the formation water in the aquifer.

Parameter	Value	Elements	Concentration (M)
Temperature (°C)	37	Al	1.30×10^{-8}
pH	7.67	C	2.98×10^{-3}
		Ca	7.11×10^{-3}
		Cl	5.25×10^{-1}
		K	4.26×10^{-4}
		Mg	9.58×10^{-2}
		Na	3.11×10^{-1}
		Si	2.53×10^{-4}

equilibrium constants are tabulated for any reactions based on eight temperatures. No pressure dependent corrections were implemented.

2.4.3. Molecular diffusion

Our simulations considered molecular diffusion in a single aqueous phase as the dominant mass transport process. We assumed stagnant conditions in the modelled system (no net flow of brine). This assumption is strictly only valid in the cap rock. In the aquifer, relatively high porosity and permeability conditions allow mass transfer to occur by advection in response to local hydraulic gradients, but the flow in the cap rock – the focus of this study – would still be negligible (Bear, 1972).

The mass transport process in the cap rock can be treated based on Fick's first law, where the diffusive flux is proportional to the concentration gradient:

$$J_i = -D^i_{eff} \frac{\partial C_i}{\partial x} \tag{4}$$

where C_i is the concentration of the diffusing species in solution and D^i_{eff} is its effective diffusion coefficient, and x is the distance. The effective diffusion coefficient can be thought of as the product of the diffusion coefficient of the species in an aqueous solution at infinite dilution and a formation factor that accounts for the spatial variations in porosity (ϕ) and tortuosity (τ) of the transport paths. Tortuosity attempts to account for the longer distance traversed in pores compared to a straight-line distance (Cussler, 2009) and is a parameter which allows an effective diffusion coefficient in the porous medium to be calculated from the diffusion coefficient in pure water (d_w) and the porosity according to the following equation:

$$D^i_{eff} = \phi \frac{d_w}{\tau} \tag{5}$$

where ϕ is the porosity, d_w is the diffusion coefficient in pure water, and τ is the tortuosity. The diffusion model used the same pure water diffusion coefficient applied for all dissolved species (1×10^{-9} m^2/s). We assume there are no different tracer diffusivities for the species and no electrochemical migration effects due to the different charges of various ions. This assumption is in line with previous work (Giambalvo et al., 2002; Boudreau et al., 2004). In this model, the initial porosity of cap rock was 0.15. Tortuosity usually ranges between 2 and 6, averaging approximately 3 (Cussler, 2009), the value used in our model. Thus, by assuming a fixed diffusion coefficient for all aqueous species in Tables 1 and 3 as 1×10^{-9} m^2/s and a tortuosity of 3, the calculated effective diffusion coefficient for all aqueous species is 3.33×10^{-10} m^2/s.

3. Results and discussion

3.1. Kinetic batch modelling

Kinetic batch modelling simulates the reaction of mixed species with no diffusion for 10,000 years. The initial fugacity, f_{CO_2}, of pure CO_2 is 52 atm. The initial fugacity of CO_2 decreases with an increase in CH_4 concentration. In this simulation, the migration of CO_2 over time and spatial scales due to flow and diffusion was not considered. The results

are discussed with respect to pH, mineral dissolution/precipitation, and porosity.

3.1.1. pH

Following the injection of CO_2 into the system, the pH immediately decreases from 7.7 to below 4 (Fig. 3A), and thereafter gradually increases to 5.8 at the end of 10,000 years. After ten years, the pH for reactions with rock assemblages decreases with increasing initial fugacity. This is due to the increase of dissolved CO_2 in the brine and the pH is not completely neutralized by reactions with carbonate minerals.

The initial f_{CO2} controls the available CO_2 in the system and consequently the evolution of the pH over the course of the reaction. A small amount of CH_4 decreases the initial fugacity of CO_2 making the brine less acidic. The dissolution and precipitation of the minerals, discussed below, reflect the consumption of the acidic CO_2 by CO_2–brine–mineral reactions. These geochemical reactions result in an increasing pH at later stages. A higher initialf_{CO2} increases the amount of dissolved CO_2 in the brine, and as a result increases the extent of mineral dissolution. Minerals such as calcite dissolve rapidly, leading to an increase in pH and porosity. After 1000 years of reaction (Fig. 3B), the pH of the aqueous solution does not change significantly. This is because equilibrium has been attained once all of the CO_2 has dissolved into the brine and reacted with the minerals.

3.1.2. Mineral dissolution/precipitation

The dissolved CO_2 in brine after injection causes minerals to dissolve and precipitate. Figs. 4 to 14 show the masses of individual minerals dissolved and precipitated over time for the kinetic batch modelling. Fig. 4 shows that a small quantity of calcite dissolves rapidly during the first 100 years and equilibrates with the brine according to **reactions 1 and 2**, (Table 4). Much of the bicarbonate formed from the dissolution of CO_2 is removed from the brine by precipitation of dolomite. In addition, a small amount of siderite precipitates. K-feldspar and albite dissolves and calcite and dawsonite precipitates. The dissolution of albite and K-feldspar canbe presented by **reactions 3 and 4**. The formation of calcite and dawsonite can be presented by **reactions 5 and 6**.

Dissolution of K-feldspar over 10,000 years (Fig. 5) contributes Al^{3+} to the solution, which reacts with Na^+ in the initial brine and dissolved

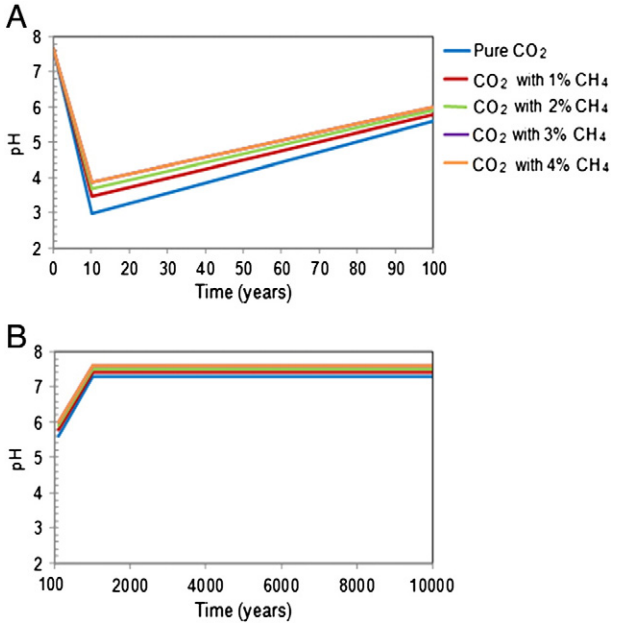

Fig. 3. Evolution of the pH for kinetic batch modelling of dissolved CO_2 in the cap rock with 0, 1, 2, 3, and 4 (w/w)% CH_4. (a) Short-term reactions (0–100 years). (b) Long term reactions (100–10,000 years). The initial fugacity, f_{co2} controls the available CO_2 in the system. A small amount of CH_4 decreases the initial fugacity of CO_2resulting in less acidic brine.

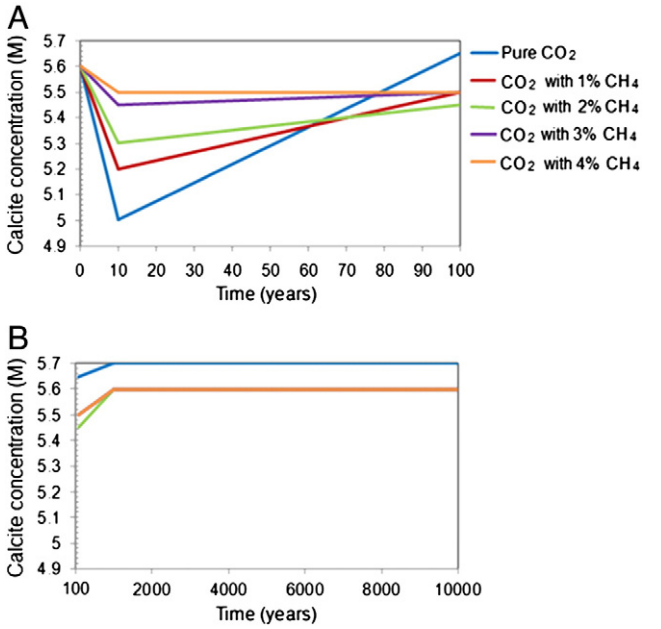

Fig. 4. Dissolution and precipitation of calcite in the rock for kinetic batch modelling of dissolved CO_2 in the cap rock with 0, 1, 2, 3, and 4 (w/w)% CH_4. (a) Short-term reactions (0–100 years). (b) Long term reactions (100–10,000 years).

CO_2 to form dawsonite. Dissolution of albite (Fig. 6) and K-feldspar is driven by the decrease in pH due to dissolved CO_2. The dissolution of aluminosilicate minerals buffers the pH and provides Na^+ and Al^{3+} needed for precipitation of carbonate minerals such as dawsonite (Fig. 7). The precipitation of calcite and dawsonite is controlled by the dissolution rate of the initial mineral composition represent of calcite, albite, K-feldspar, and other aluminosilicates. Calcite, albite, and K-feldspar dominate the short term reactions, whereas aluminosilicate dominate long term reactions.

The most important precipitation of secondary carbonates upon CO_2injection are calcite ($CaCO_3$) and dawsonite ($NaAlCO_3[OH]_2$). Precipitation of these carbonate minerals requires sufficient amounts of Ca^{2+} and Na^+available. In addition, Al^{3+} needs to be available in the formation water. These ions are added to the brine by dissolution of calcite and aluminosilicates resulting from the high acidity after CO_2 injection. Since the aquifer is highly saline, the Na^+ needed for dawsonite precipitation is available in the initial brine. Additional Na^+ and Al^{3+} are obtained through dissolution of albite and K-feldspar. Dissolution of these aluminosilicates minerals neutralizes the acidic brine.

Leaching of Ca^{2+} and Na^+, two important cations with respect to dissolution and precipitation of calcite and dawsonite, are shown in Figs. 8 and 9. As seen in Fig. 8, after a slight increase during the first ten years, the molality of Ca^{2+} decreases gradually before it stabilizes at concentrations between 0.18, 0.168, 0.165, and 0.16 M for pure CO_2,

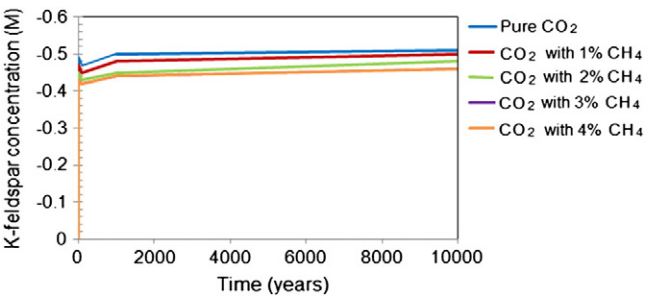

Fig. 5. Dissolution of K-feldspar for kinetic batch modelling of dissolved CO_2 in the cap rock with 0, 1, 2, 3, and 4 (w/w)% CH_4. The initial concentration of K-feldspar in the rock is 4.08 mol/l of brine. Negative values indicate net dissolution of K-feldspar in the rock.

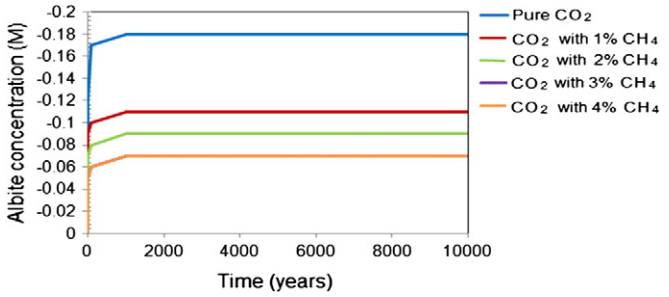

Fig. 6. Dissolution of albite for kinetic batch modelling of dissolved CO_2 in the cap rock with 0, 1, 2, 3, and 4 (w/w)% CH_4. The initial concentration of albite in the rock is 25.6 mol/l of brine. Negative values indicate net dissolution of the albite in the rock.

CO_2 with 1% CH_4, CO_2 with 2%, and CO_2 with 3% CH_4, and CO_2 with 4% CH_4, respectively. Fig. 9 shows a significant decrease of Na^+ concentration with increasing CH_4 percentage. The Na^+ concentration peaks at approximately 100 years (Fig. 9A) and later gradually decreases reaching concentrations of approximately 0.173, 0.165, and 0.163 and 0.16 M for pure CO_2 and CO_2 with 1% CH_4, CO_2 with 2% CH_4, CO_2 with 3% CH_4, and CO_2 with 4% CH_4 at 10,000 years, respectively (Fig. 9B).

Calcite and dawsonite precipitate in alkaline solutions as more Na^+ and HCO_3^- are available. Thus, with the increased total concentration of Ca^{2+} obtained from the dissolution of calcite, the precipitation of secondary carbonates, calcite and dawsonite, is favoured. Other than that, minor precipitation of siderite ($FeCO_3$) and magnesite ($MgCO_3$) are observed. The available Fe^{2+} (Fig. 10) and Mg^{2+} (Fig. 11) from the dissolution of illite $(K,H_3O)(Al,Mg,Fe)_2((Si,Al)_4O_{10}[(OH)_2,(H_2O)]$ (Fig. 12), when the brine becomes acidic due to perturbation of CO_2 into the cap rock trigger the formation of siderite and magnesite (Figs. 13 and 14). The dominant reaction in the system over 10,000 years is the dissolution of albite ($NaAlSi_3O_8$). Apart from the precipitation of dawsonite, the dissolution of albite leads to the formation of kaolinite (Al_2SiO_5 $(OH)_4$).

The precipitation of ankerite ($CaMg_{0.3}Fe_{0.7}(CO_3)_2$) requires the presence of Ca^{2+}, Mg^{2+}, and Fe^{+2}. This is supplied by calcite ($CaCO_3$), chlorite ($Mg_{2.5}Fe_{2.5}Al_2Si_3O_{10}(OH)_8$) or by dissolution of hematite (Fe_2O_3)

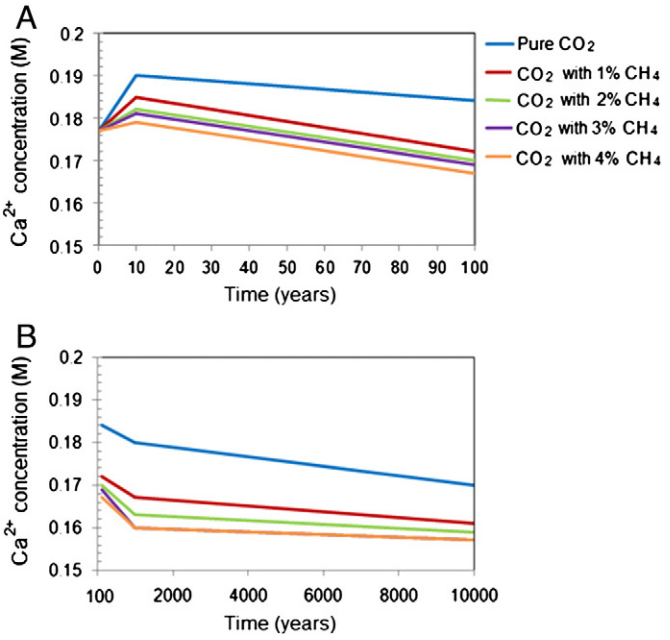

Fig. 8. Kinetic batch modelling of dissolved CO_2 in the cap rock with 0, 1, 2, 3, and 4 (w/w)% CH_4. (a) Evolution of Ca^{2+} in the brine during short-term reactions (0–100 years). (b) Evolution of Ca^{2+} in the brine during long-term reactions (100–10,000 years).

and subsequent reduction of the ferric iron. Precipitation of ankerite itself is not considered in our models because the primary mineral of the cap rock does not include chlorite and hematite.

3.2. Molecular diffusion modelling

We now consider geochemical reactions coupled with transport. Since transport occurs only by diffusion, it is possible to estimate the minimum time necessary for a solute to diffuse across the domain. The time taken to diffuse a distance x for all aqueous species in Tables 1 and 2 is approximated by x^2/D with an effective diffusion

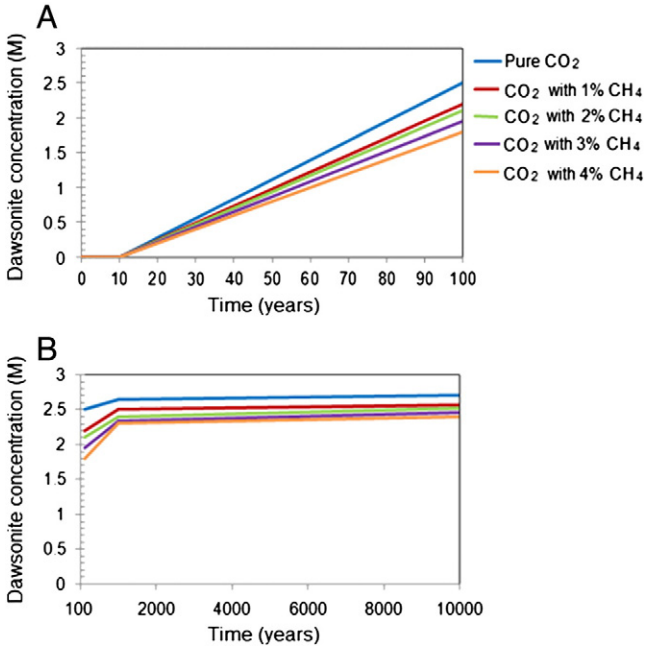

Fig. 7. Precipitation of dawsonite for kinetic batch modelling of dissolved CO_2 in the cap rock with 0, 1, 2, 3, and 4 (w/w)% CH_4. Dawsonite is a secondary mineral. (a) Short-term reactions (0–100 years). (b) Long term reactions (100–10,000 years).

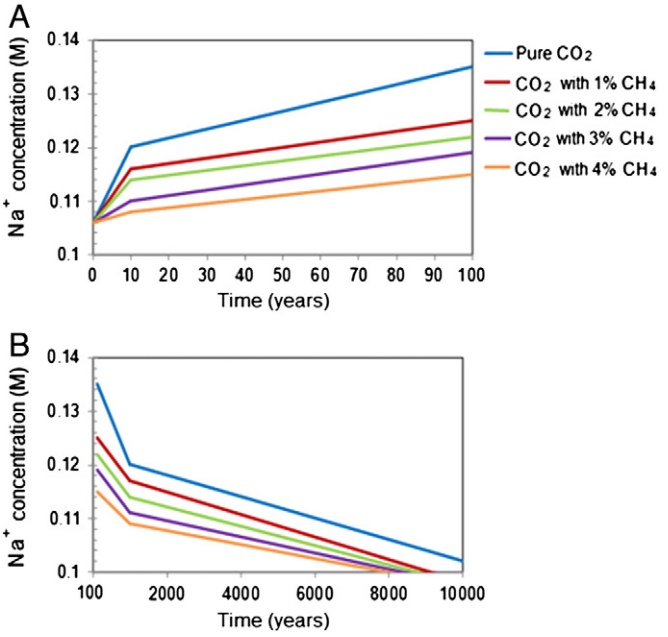

Fig. 9. Kinetic batch modelling of dissolved CO_2 in the cap rock with 0, 1, 2, 3, and 4 (w/w)% CH_4. (a) Evolution of Na^+ in the brine during short-term reactions (0–100 years). (b) Evolution of Na^+ in the brine during long-term reactions (100–10,000 years).

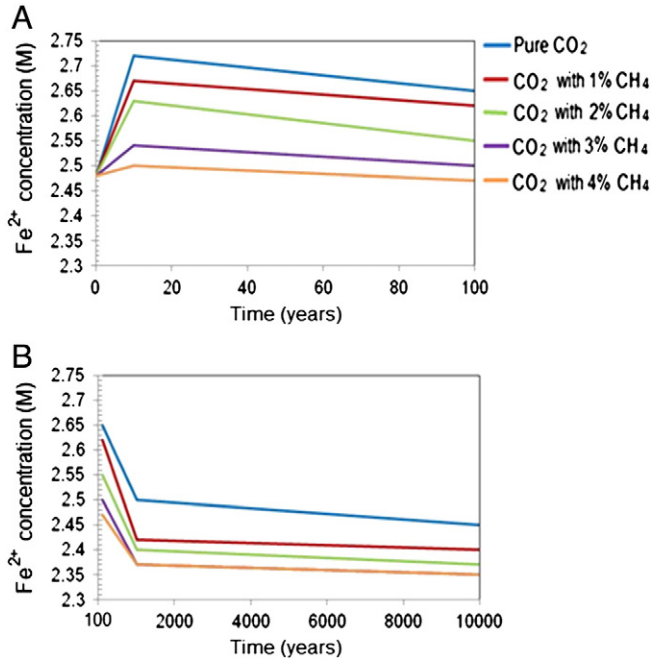

Fig. 10. Kinetic batch modelling of dissolved CO_2 in the cap rock with 0, 1, 2, 3, and 4 (w/w)% CH_4. (a) Evolution of Fe^{2+} in the brine during short-term reactions (0–100 years). (b) Evolution of Fe^{2+} in the brine during long-term reactions (100–10,000 years).

coefficient $D = 3.33 \times 10^{-10}$ m^2/s. Noting that one year is approximately 3×10^7 s, we find a time of around 100 years to travel one grid block (1 m) and 10,000 years to traverse the whole system (10 m).

3.2.1. pH

Sulphate may very well be present under anoxic conditions as the conversion from sulphate to sulphide requires microbial reduction by sulphate reducing bacteria, which may be coupled to methane oxidation (Joye, 2012). Sulphate in the brine reacts with methane during

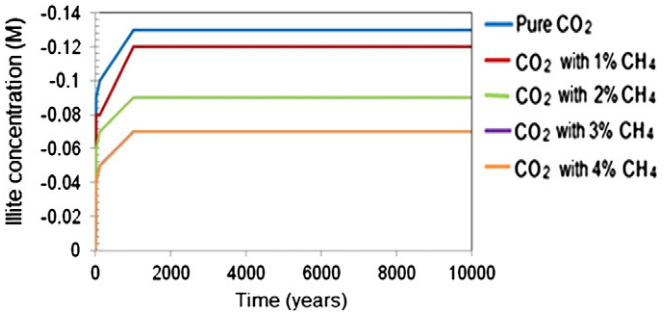

Fig. 12. Dissolution of illite for kinetic batch modelling of dissolved CO_2 in the cap rock with 0, 1, 2, 3, and 4 (w/w)% CH_4. The initial concentration of illite in the rock is 35.21 mol/l of brine. Negative values indicate net dissolution of the illite in the rock.

anaerobic methane oxidation (AMO) (**reaction 7**, Table 4). AOM is a metabolic process (Hoehler et al., 1994) mediated in marine environments by associations between anaerobic methanotrophic archaea (Hinrichs et al., 1999) and sulphate-reducing bacteria. The archaea are not bacterial/microorganisms, but a domain of single-celled microorganisms. During AMO, methane is oxidized with sulphate as the terminal electron acceptor. The production of bicarbonate from AMO results in the precipitation of calcium carbonate or known as authigenic carbonate (**reaction 7**, Table 4). This mechanism limits the acidification of the cap rock when methane is present.

For a pure CO_2 stream, the effect on the pH is limited to within of 8 m in the cap rock above the aquifer interface (Fig. 15A) after 10,000 years. For CO_2 with 1% CH_4, the effect on the pH is contained within only 5 m of the cap rock (Fig. 15B). The migration distance of acidic brine decreases with an increase in the amount of admixed CH_4 (Fig. 15). This is in agreement with the observations of the kinetic batch model (see above) where CH_4 reduces the changes in pH. The migration distance is less than that permitted by diffusion alone, and so the brine is buffered in the presence of CH_4 which limits the movement of the protons in the system.

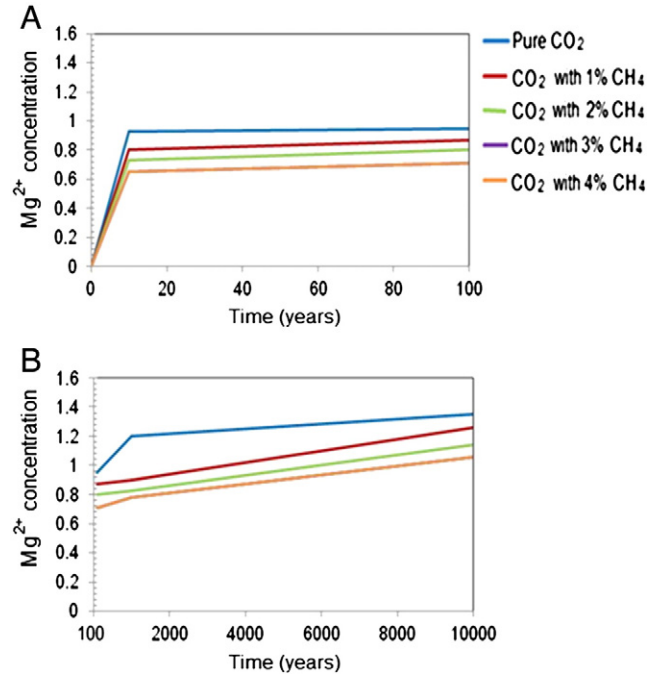

Fig. 11. Kinetic batch modelling of dissolved CO_2 in the cap rock with 0, 1, 2, 3, and 4 (w/w)% CH_4. (a) Evolution of Mg^{2+} in the brine during short-term reactions (0–100 years). (b) Evolution of Mg^{2+} in the brine during long-term reactions (100–10,000 years).

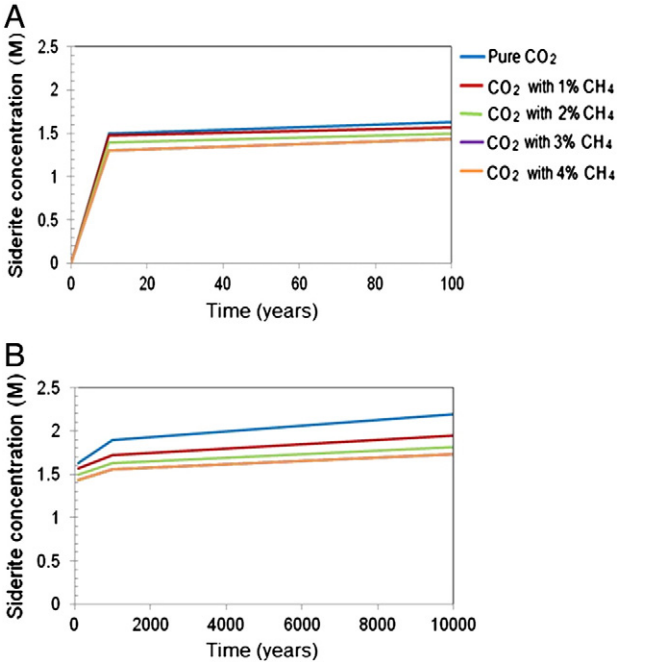

Fig. 13. Precipitation of siderite for kinetic batch modelling of dissolved CO_2 in the cap rock with 0, 1, 2, 3, and 4 (w/w)% CH_4. The initial concentration of siderite in the rock is 8.60 mol/l of brine. (a) Short-term reactions (0–100 years). (b) Long term reactions (100–10,000 years).

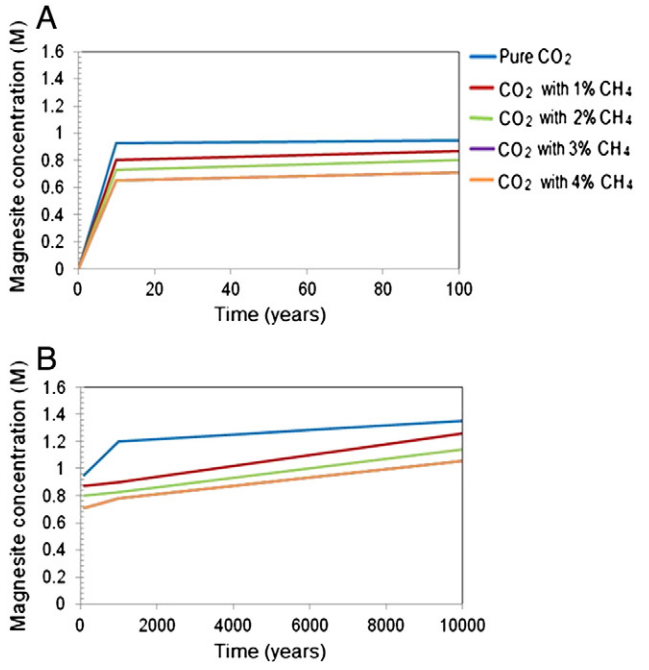

Fig. 14. Precipitation of magnesite for kinetic batch modelling of dissolved CO_2 in the cap rock with 0, 1, 2, 3, and 4 (w/w)% CH_4. Magnesite is a secondary mineral. (a) Short-term reactions (0–100 years). (b) Long term reactions (100–10,000 years).

3.2.2. Mineral dissolution/precipitation

The process controlling the geochemical reactions of the system is the dissolution/precipitation of calcite (**reactions 2 and 4**, Table 4). Calcite dissolves under acidic conditions and precipitates under alkaline conditions as observed in the batch simulations of the previous section. This also is also seen in Fig. 16, where calcite dissolves the lower part in the cap rock and precipitates in the upper part of the column. Fig. 16 shows the changes in the volume fraction of calcite. Dissolution of calcite in the first few cells of the cap rock is driven by low pH conditions induced by the high partial pressure of CO_2, P_{CO_2}, in the aquifer. Calcite dissolution increases the available concentration of Ca^{2+} in the cap rock brine. The high concentration of Ca^{2+} diffuses from the lower part to the upper part of the cap rock column due to the concentration gradient vertically. This induces an upward movement of Ca^{2+} through the column.

Calcite dissolution/precipitation reactions are expressed using the calcite saturation index calculated using:

$$SI = log(IAP/K) \quad (6)$$

Where IAP is the ion activity product and K is the solubility product. For pure CO_2, after 100 years of reaction, the simulations show that calcite is highly under saturated ($SI < 0$) in the lower 2 m of the cap rock, and slightly oversaturated in the cap rock cells above (Fig. 16). This oversaturation triggers the precipitation of calcite. On the other hand, CO_2 with 1–4 (w/w)% CH_4 results in solutions highly under saturated with respect to calcite ($SI < 1$) in less than 1 m at the lower part of the cap rock column (Fig. 16B, C, and D) and the amount of dissolved calcite decreases in this region at late time. Beyond the region 1 m, calcite is slightly oversaturated ($SI > 0$).

The diffusive flux of Ca^{2+} leads to precipitation of calcite and this seals the void spaces in the upper cells in the cap rock column. This process is dominant over the competing diffusion of protons (H^+) induced by acidification in the aquifer. The mineral assemblages in the cap rock act as a buffer that inhibits propagation of the acid front created by high P_{CO2} conditions in the aquifer. In this model, however, we do not alter the diffusion coefficient as the porosity changes, but keep it fixed at its initial value.

The dissolution/precipitation behaviour of minerals other than calcite such as dawsonite does not significantly control the porosity during the first 100 years. Dawsonite might play a significant role in controlling the composition of the aqueous solution for longer time periods, beyond 10,000 years (Fig. 17).

3.2.3. Porosity

The geochemical reactions after CO_2 injection result in increased porosity in the cap rock in the lower part of the cap rock (less than 10 m). The changes of porosity can be calculated from changes in volume of minerals. The dissolution of primary and precipitation of secondary minerals such as calcite changes the formation porosity which alters the fluid flow pattern.

Porosity changes are shown in Fig. 18. The increase is caused by the acidic brine that triggers the dissolution of minerals such as calcite and albite. The dissolution of these minerals increases the concentration of Ca^{2+} and Na^+ in the brine. High concentrations of these ions lead to the precipitation of calcite and dawsonite in the upper part of the cap rock. This improves the cap rock sealing security. Overall there is a smaller increase in porosity as the CH_4 concentration increases, indicating that this impurity in the injection stream leads to improved storage security.

3.3. Grid refinement

We also ran a model with half the grid spacing – 0.05 m – and obtained essentially identical results. This suggests that our results are not sensitive to numerical dispersion and other errors in the discretization of the transport and reaction equations.

3.4. Model validations

Our simulations suggest that precipitation of secondary minerals such as calcite and dawsonite upon CO_2 injection into the aquifer play a vital role in sealing capacity of the cap rock. Here, we assess our

Table 4
The chemical reactions considered in this study.

Reaction 1
Dissolution of CO_2: $H_2O + CO_{2(g)} \rightleftarrows H_2CO_3^- \rightleftarrows H^+ + HCO_3^-$
Reaction 2
Calcite dissolution: $CaCO_3 + H^+ \rightleftarrows Ca^{2+} + HCO_3^-$
Reaction 3
Albite dissolution: $2Na(AlSi_3)O_8 + 2H^+ + 9H_2O \rightleftarrows Al_2Si_2O_5(OH)_4 + 2Na^+ + 4H_4SiO_4$
Reaction 4
K-feldspar dissolution: $KFe_3AlSi_3O_{10}(OH)_2 + 7CO_2 + H_2O \rightleftarrows 3FeCO_3 + 3SiO_2 + K^+ + 4HCO_3^- + Al^{3+}$
Reaction 5
Calcite precipitation: $2NaAlSi_3O_8 + CO_2 + 2H_2O + Ca^{2+} \rightleftarrows 4SiO_2 + CaCO_3 + Al_2Si_2O_5(OH)_4 + 2Na^+$
Reaction 6
Dawsonite precipitation: $NaAlSi_3O_8 + CO_2 + H_2O \rightleftarrows 3SiO_2 + NaAlCO_3(OH)_2$
Reaction 7
Anaerobic methane oxidation: $CH_4 + SO_4^{2-} \rightleftarrows HCO_3^- + HS^- + H_2O$

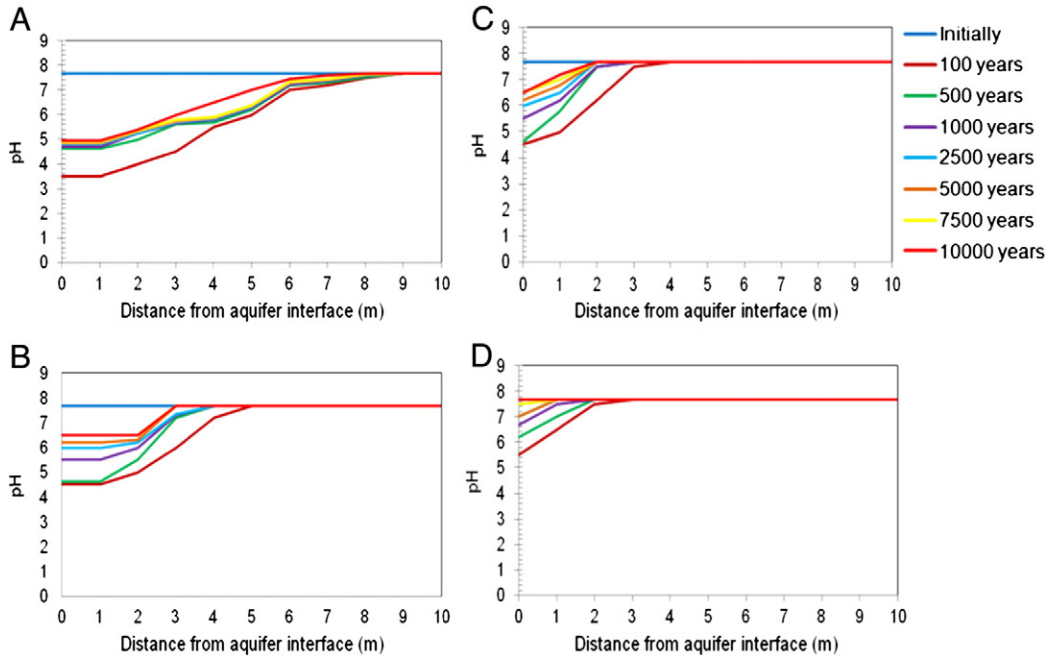

Fig. 15. Diffusion of the acidified aquifer brine: pH profiles in the cap rock over 10,000 years. Porosity is 0.15, the effective diffusion coefficient D_{eff}^{i} is 3.33×10^{-10} m^2/s. (a) Injection of pure CO_2. (b) Injection of CO_2 with 1 (w/w)% CH_4. (c) Injection of CO_2 with 2 (w/w)% CH_4. (d) Injection of CO_2 with 4 (w/w)% CH_4.

model findings in the light of experimental laboratory evidence, numerical simulations, and field observations from natural analogues.

3.4.1. Comparison with laboratory experiments

The reactivity of cap rock with fluids after CO_2 injection has been tested in laboratory experiments (Kaszuba et al., 2005; Angeli et al., 2009; Credoz et al., 2009; Alemu et al., 2011) and we find good qualitative agreement with our results. Alemu and co-workers conducted batch dissolution experiments with shale using a mixture of CO_2 and brine fluids at temperatures between 80 and 250 °C and a pressure of 110 bars for one to five weeks (Alemu et al., 2011). The shale samples were sourced from the Adventalen group overlying a proposed underground CO_2 storage site in Svalbard, near Longyearbyen, Norway. After the dissolution of CO_2, XRD and SEM analyses showed significant dissolution of primary minerals such as primary carbonates, chlorite and illite, and precipitation of secondary minerals such as smectitie and calcite. Ingression of CO_2 significantly reduced the pH and increased the reaction rates.

Batch reactions were also conducted by Credoz and co-workers using two cap rock samples from the Chinle Shale, western USA, and

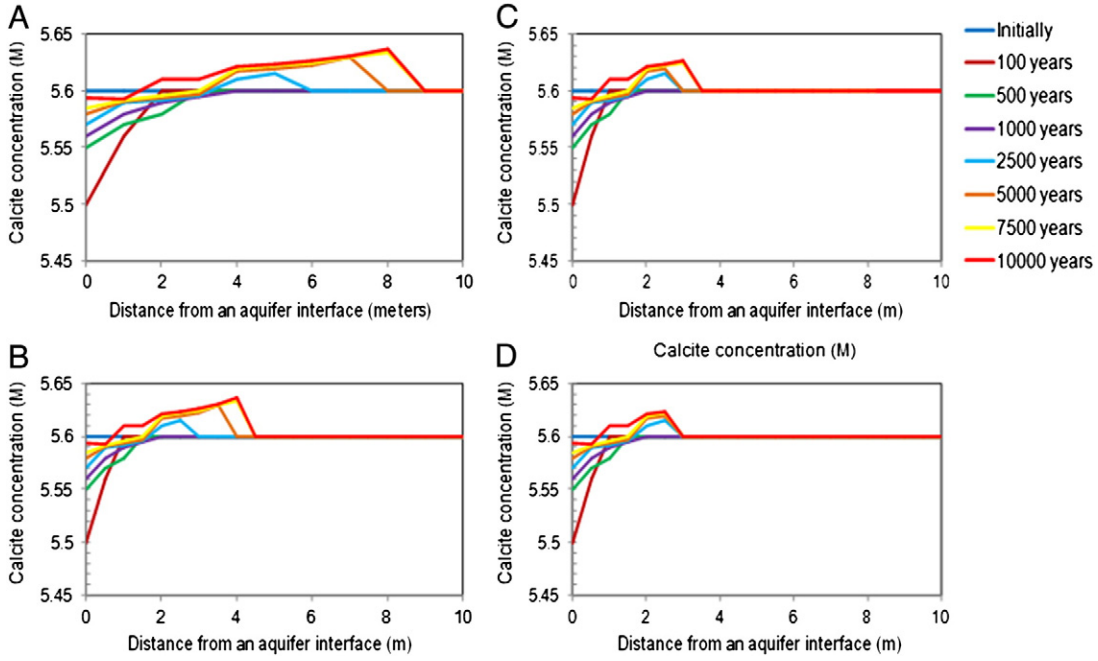

Fig. 16. Concentration of calcite in the rock over a distance of 10 m through the cap rock column. The simulation was run for 10,000 years. The initial calcite concentration is 5.6 M and decreases initially as calcite dissolves and enters the aqueous phase. Later the concentration increases due to precipitation. (a) Injection of pure CO_2. (b) Injection of CO_2 with 1 (w/w)% CH_4. (c) Injection of CO_2 with 2 (w/w)% CH_4. (d) Injection of CO_2 with 3 and 4 (w/w) % CH_4.

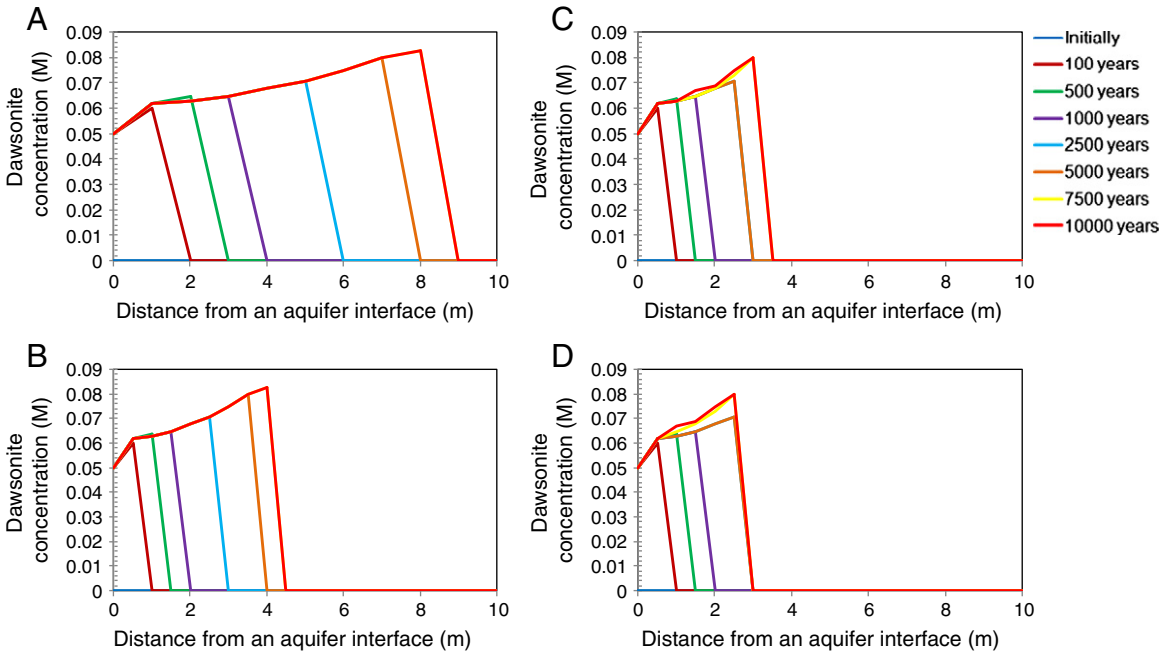

Fig. 17. Concentration of dawsonite in the rock over a distance of 10 m through the cap rock column. The simulation was run for 10,000 years. The initial dawsonite concentration is 0 M. Dawsonite is treated as a secondary mineral. (a) Injection of pure CO_2. (b) Injection of CO_2 with 1 (w/w)% CH_4. (c) Injection of CO_2 with 2 (w/w)% CH_4. (d) Injection of CO_2 with 3 and 4 (w/w) % CH_4.

from the Comblanchien Formation, Paris basin, France (Credoz et al., 2009). The experiments were conducted for one year at temperatures between 80 and 150 °C and pressures of 1 and 150 bars. XRD and SEM analyses showed dissolution of carbonates at low temperature and precipitation of mixed carbonates (Fe^{2+}, Ca^{2+}, Mg^{2+}) and smectite at higher temperature (150 °C). At the end of the experiments, the dissolution of carbonates buffered the fluid pH between 6.3 and 8. The concentration of Ca^{2+}, Mg^{2+}, and K^{+} increased by approximately 50%. The high concentrations triggered the precipitation of secondary minerals. Our simulation results showed a similar increase in concentration of two major ions: Ca^{2+} and Na^{+}. Higher concentrations of these ions are due to the dissolution of initial calcite and albite in the cap rock. The dissolution of these minerals was triggered by acidic brine from dissolution of CO_2.

With respect to the dissolution of clay minerals in cap rock model, studies conducted on smectite (Rozalén et al., 2008, 2009) and illite (Bibi et al., 2011) minerals suggest that the dissolution rates increase with rising acidity.

Kaszuba and co-workers conducted batch dissolution experiments using mixed aquifer (synthetic arkose) and aquitard (Silurian shale) samples at 200 °C and 200 bars The shale samples reacted with 5.5 M NaCl brine for a period of 32 days before injection of CO_2 and the

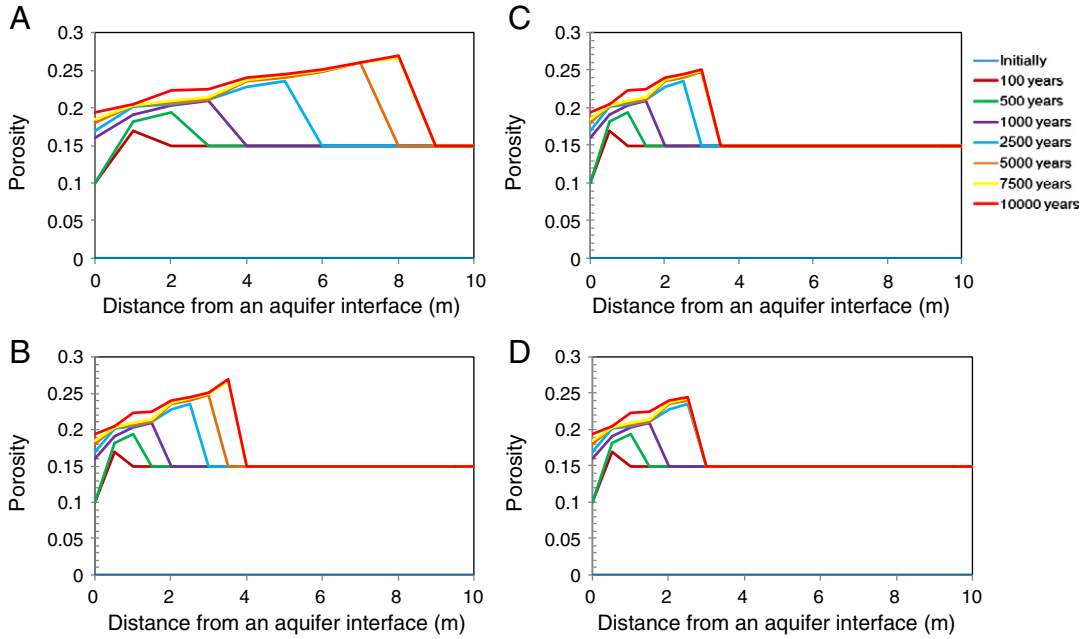

Fig. 18. Porosity changes over a distance of 10 m through the cap rock column. The initial porosity is 0.15. (a) Injection of pure CO_2. (b) Injection of CO_2 with 1 (w/w)% CH_4. (c) Injection of CO_2 with 2 (w/w)% CH_4. (d) Injection of CO_2 with 3 and 4 (w/w) % CH_4.

reaction continued for 45 days. Primary minerals such as siderite dissolved following the decrease of pH after CO_2 injection. The low pH was buffered by the mineral phases, which restored the pH to almost neutral values. This is in line with our simulation at a lower temperature (37 °C) and pressure (100 bars), which showed rapid dissolution of calcite and siderite during CO_2 injection. However, these minerals re-precipitate in large amounts later due to the increase of Ca^{2+} and Fe^{2+} concentrations in brine. These reactions create the buffering conditions in the system.

The experiments discussed were conducted at high temperatures to accelerate silicate reactions in the cap rock and the precipitation of dawsonite was rarely observed. This is in contrast to our and other modelling results where precipitation of dawsonite is observed (Gaus et al., 2005). The differences are explained by factors such as kinetic and nucleation effects that likely prevent the formation of these minerals over the short time scales of the laboratory experiments (Hellevang et al., 2011). The precipitation of secondary silicate minerals such as dawsonite is likely to take thousands of years (Hellevang et al., 2005).

3.4.2. Comparisons with modelling work

Reactive transport modelling of the cap rock sealing capacity due to CO_2 injection into saline aquifers has been performed before (Gaus et al., 2005; Gherardi et al., 2007). These simulations show evidence of calcite and dawsonite precipitation in the upper zone of the cap rock. The initial mineralogy temperature (37 °C) and pressure (100 bar) used in this works were similar, but the reaction times were 3000 years compared to our 10,000 years. The main difference between the model of Gaus et al. (2005) and ours is the choice of the effective diffusion coefficients and the inclusion of tortuosity values. Gaus et al. (2005) assumed an average value for diffusion coefficient of 10^{-9} for all of aqueous species. Our study considered the tortuosity factor and calculated the effective diffusion coefficient. Despite these differences, the formation of calcite after 10 years in the upper part of the cap rock column is observed in both models. The higher concentrations of Ca^{2+} lead to calcite precipitation. The presence of methane impurities was also not considered in that study (Gaus et al., 2005).

3.4.3. Comparison with natural analogues

Various investigations have studied source, migration, and fate of naturally occurring CO_2 in gas fields using noble gas and stable carbon isotope tracers (Baines and Worden, 2004; Moore et al., 2005; Gilfillan et al., 2008, 2009; Worden and Burley, 2009). The results suggest that dissolution of host rocks in formation brine at pH between 5 and 5.8 is the primary sink for CO_2. Work on the integrity of mud rock seal overlying a natural CO_2 reservoir in the North Sea Miller oil field (Lu et al., 2009) showed the significant presence of CO_2gas in the basal cap rock compared to dissolved CO_2 and evidence of precipitation of secondary minerals.

The formation of secondary minerals suggested from our modelling is in line with observations of dawsonite formation as secondary minerals after dissolution of plagioclase in the Permian Supai Formation of the Springerville-St. John CO_2 field associated with magmatic or volcanic activity (Moore et al., 2005). Aqueous species sampled from this site showed a drop in total inorganic compounds resulting from formation of secondary carbonate phases such as calcite and dawsonite. Other fields that observed formation of dawsonite are Bowen, Gunnedah, the Sydney Basins of New South Wales (Baker et al., 1995) and Denison Trough of east-central Queensland (Baker, 1991; Baker and Decaritat, 1992).

4. Discussion and conclusions

A homogenous kinetic batch and one-dimensional kinetically controlled molecular diffusion modelled expected physical and chemical processes in the cap rock of a storage site (Sleipner). Our study addressed the effect of pure CO_2 and 1–4 (w/w)% CH_4 contaminated CO_2 stream on cap rock sealing capacity. The integrity of the cap rock was assessed from the dissolution/precipitation of minerals on porosity changes. The porosity was calculated from changes in mineral volume.

The major conclusions from this study can be divided into two aspects: kinetic batch reactions modelling and molecular diffusion modelling. Findings from kinetic batch modelling show that the presence of CH_4 suppresses the dissolution/precipitation of minerals. The presence of CH_4 (1–4 (w/w)%) in the system decreases the acidity of the brine. As a result, this affects the dissolution rate of minerals such as calcite.

For molecular diffusion modelling, the conclusions are as follows:

1) The distance from the aquifer that is affected is limited to less than 8 m for pure CO_2 and 5 m for mixtures of CO_2 with CH_4 (1–4 (w/w)%) over a timescale of 10,000 years. This is less than the maximum distance that the solute can move by diffusion, 10 m, and implies buffering of the brine. The migration of acidic brine through the cap rock is reaction limited.
2) Dissolution of calcite during short term reactions (0–100 years) increases the porosity in the cap rock. As a result, this may enable CO_2-rich fluids to migrate upwards in the cap rock.
3) The dominant role played by calcite is due to its fast kinetic rates and overwhelms the dissolution/precipitation of other minerals during short-term reactions (0–100 years). However, over longer times, the effect of dawsonite precipitation overwhelms other mineral dissolution/precipitation. This is due to the dissolution of albite that contributes to the high concentrations of Na^+ in the brine for dawsonite precipitation.
4) The presence of CH_4 decreases the initial partial pressure (fugacity) of CO_2. This causes the brine to be less acidic and causes less reaction. Thus, the acidic brine front moves slower with a more modest change in porosity.
5) Both pure CO_2 and mixtures of CO_2 with CH_4 in the injected gas decrease the porosity of the cap rock in the long term. This enhances the sealing capacity of the cap rock.
6) The model suggests that co-injection of CO_2 with CH_4 could provide safer storage than injecting pure CO_2 while reducing separation costs. The CH_4 limits the migration of acidic brine and calcite, ensuring that the cap rock remains unaffected by injection. This needs to be balanced against the lower injected phase density and greater storage volume required.

Further improvement to the reactive transport simulator; PHREEQC 2.15.0 is required for truly predictive modelling of these geochemical processes especially in heterogeneous systems. It is suggested that further refinement of the kinetic and thermodynamic properties such as equilibrium constants on real-field data to obtained more accurate results.

The simulation results presented in this paper are only specific to the conditions studied: a temperature of 37 °C and a pressure of 100 bar, with the other parameters considered. Thus, it is recommended to re-run these tools to study other specific storage sites, using the pertinent conditions. However, reactive transport modelling tools are still the best options for analysing and evaluating the reliability of cap rock in the absence of direct, long-term laboratory data.

Acknowledgements

The authors acknowledge the Ministry of Higher Education of Malaysia, University of Malaya, Malaysia for financial support and the thorough reviews of Syed AmerShafiuddin and two anonymous reviewers.

References

Alemu, B.L., Aagaard, P., Munz, I.A., Skurtveit, E., 2011. Caprock interaction with CO_2: a laboratory study of reactivity of shale with supercritical CO_2 and brine. Appl. Geochem. 26 (12), 1975–1989.

Angeli, M., Soldal, M., Skurtveit, E., Aker, E., 2009. Experimental percolation of supercritical CO_2 through a cap rock. Energy Procedia 1 (1), 3351–3358.

Appelo, C.A.J., Postma, D., 2005. Geochemistry, Groundwater and Pollution. A.A. Balkema (649 pp.).

Austegard, A., Solbraa, E., De Koeijer, G., Molnvik, M.J., 2006. Thermodynamic models for calculating mutual solubilities in H_2O–CO_2–CH_4 mixtures. Chem. Eng. Res. Des. 84 (A9), 781–794.

Baines, S.J., Worden, R.H., 2004. The long-term fate of CO_2 in the subsurface: natural analogues for CO_2 storage. Geol. Soc. Lond. Spec. Publ. 233 (1), 59–85.

Baker, J.C., 1991. Diagenesis and reservoir quality of the Aldebaran sandstone, Denison Trough, East-Central Queensland, Australia. Sedimentology 38 (5), 819–838.

Baker, J.C., Decaritat, P., 1992. Postdepositional history of the Permian sequence in the Denison Trough, Eastern Australia. AAPG Bull. 76 (8), 1224–1249.

Baker, J.C., Bai, G.P., Hamilton, P.J., Golding, S.D., Keene, J.B., 1995. Continental-scale magmatic carbon-dioxide seepage recorded by dawsonite in the Bowen–Gunnedah–Sydney Basin System, Eastern Australia. J. Sediment. Res. 65 (3), 522–530.

Baklid, A., Korbol, R., Owren, G., 1996. Sleipner vest CO_2 disposal, CO_2 injection into a shallow underground aquifer. SPE Annual Technical Conference and Exhibition, Denver, Colorado, USA, pp. 269–277.

Bear, J., 1972. Dynamics of Fluids in Porous Media. American Elsevier Pub. Co.

Bertier, P., Swennen, R., Laenen, B., Lagrou, D., Dreesen, R., 2006. Experimental identification of CO_2–water–rock interactions caused by sequestration of CO_2 in Westphalian and Buntsandstein sandstones of the Campine Basin (NE-Belgium). J. Geochem. Explor. 89 (1–3), 10–14.

Bibi, I., Singh, B., Silvester, E., 2011. Dissolution of illite in saline–acidic solutions at 25 °C. Geochim. Cosmochim. Acta 75 (11), 3237–3249.

Blum, A.E., Stillings, L.L., 1995. Chemical weathering of feldspars. In: White, A.F., Brantley, S.L. (Eds.), Chemical Weathering Rates of Silicate Minerals. Min. Soc. Am. Rev. Min, vol. 31, pp. 291–351.

BØe, R., Zweigel, P., 2001. Characterisation of the Nordland Shale in the Sleipner Area by XRD Analysis — A Contribution to the Saline Aquifer CO_2 Storage (SACS) Project.

Boudreau, B.P., Meysman, F.J.R., Middelburg, J.J., 2004. Multicomponent ionic diffusion in porewaters: Coulombic effects revisited. Earth Planet. Sci. Lett. 222 (2), 653–666.

Bowden, A.R., 2005. Assessing reservoir performance risk in CO_2 storage projects. In: Rubin, E.S., D.W.K., Gilboy, C.F. (Eds.), Greenhouse Gas Control Technologies. Elsevier.

Busch, A., et al., 2008. Carbon dioxide storage potential of shales. Int. J. Greenhouse Gas Control 2 (3), 297–308.

Credoz, A., et al., 2009. Experimental and modeling study of geochemical reactivity between clayey caprocks and CO_2 in geological storage conditions. Energy Procedia 1 (1), 3445–3452.

Cussler, E.L., 2009. Diffusion Mass Transfer in Fluid System. Cambridge University Press.

Czernichowski-Lauriol, I., et al., 1996. Inorganic geochemistry. In: Holloway, S. (Ed.), Final Report of the Joule II Project No. CT92-0031: The Underground Disposal of Carbon Dioxide. British Geological Survey, Keyworth, Nottingham, UK.

Czernichowski-Lauriol, I., Rochelle, C.A., Brosse, E., Springer, N., Bateman, K., Kervevan, C., 2002. Reactivity of injected CO_2 with the Utsira Sand reservoir at Sleipner. 6th International Conference on Greenhouse Gas Control Technology (GHGT-6), Kyoto, Japan.

De Visse, E., Hendriks, C., Barrio, M., Molnvik, M.J., De Koeijer, G., Liljemark, S., Gallo, Y.L., 2008. Dynamis CO_2 quality recommendations. Int. J. Greenhouse Gas Control 2, 478–484.

Duan, Z.H., Moller, N., Weare, J.H., 1992. An equation of state for the CH_4–CO_2–H_2O system.1. Pure systems from 0-degrees-C to 1000-degrees-C and 0 to 8000 bar. Geochim. Cosmochim. Acta 56 (7), 2605–2617.

Gao, Y.Q., Liu, L., Hu, W.X., 2009. Petrology and isotopic geochemistry of dawsonite-bearing sandstones in Hailaer basin, northeastern China. Appl. Geochem. 24 (9), 1724–1738.

Gaus, I., 2010. Role and impact of CO_2–rock interactions during CO_2 storage in sedimentary rocks. Int. J. Greenhouse Gas Control 4 (1), 73–89.

Gaus, I., Azaroual, M., Czernichowski-Lauriol, I., 2005. Reactive transport modelling of the impact of CO_2 injection on the clayey cap rock at Sleipner (North Sea). Chem. Geol. 217 (3–4), 319–337.

Gherardi, F., Xu, T., Pruess, K., 2007. Numerical modeling of self-limiting and self-enhancing caprock alteration induced by CO_2 storage in a depleted gas reservoir. Chem. Geol. 244 (1–2), 103–129.

Giambalvo, E.R., Steefel, C.I., Fisher, A.T., Rosenberg, N.D., Wheat, C.G., 2002. Effect of fluid-sediment reaction on hydrothermal fluxes of major elements, eastern flank of the Juan de Fuca Ridge. Geochim. Cosmochim. Acta 66 (10), 1739–1757.

Gilfillan, S.M.V., et al., 2008. The noble gas geochemistry of natural CO_2 gas reservoirs from the Colorado Plateau and Rocky Mountain provinces, USA. Geochim. Cosmochim. Acta 72 (4), 1174–1198.

Gilfillan, S.M.V., et al., 2009. Solubility trapping in formation water as dominant CO_2 sink in natural gas fields. Nature 458 (7238), 614–618.

Golab, A.N., Carr, P.F., Palamara, D.R., 2006. Influence of localised igneous activity on cleat dawsonite formation in Late Permian coal measures, Upper Hunter Valley, Australia. Int. J. Coal Geol. 66 (4), 296–304.

Gunter, W.D., Wiwchar, B., Perkins, E.H., 1997. Aquifer disposal of CO_2-rich greenhouse gases: extension of the time scale of experiment for CO_2-sequestering reactions by geochemical modelling. Mineral. Petrol. 59 (1–2), 121–140.

Hangx, S., Spiers, C., Peach, C., 2009. The mechanical behavior of anhydrite and the effect of CO_2 injection. Energy Procedia 1 (1), 3485–3492.

Hellevang, H., Aagaard, P., Oelkers, E.H., Kvamme, B., 2005. Can dawsonite permanently trap CO_2? Environ. Sci. Technol. 39 (21), 8281–8287.

Hellevang, H., Declercq, J., Aagaard, P., 2011. Why is dawsonite absent in CO_2 charged reservoirs? Oil Gas Sci. Technol. 66 (1), 119–135.

Hinrichs, K.-U., Hayes, J.M., Sylva, S.P., Brewer, DeLong, E.F., 1999. Nature 398, 802–805.

Hoehler, T.M., Alperin, M.J., Albert, D.B., Martens, C.S., 1994. Biogeochem. Cycles 8, 451–463.

Johnson, J.W., Morris, J.P., 2005. Reactive transport modelling of cap rock integrity during natural and engineered CO_2 storage. In: Thomas, D.C., S.M.B. (Eds.), Carbon Dioxide Capture for Storage in Deep Geologic Formations.

Johnson, J.W., Nitao, J.J., Steefel, C.I., Knauss, K.G., 2004. Reactive transport modelling of geologic CO_2 sequestration in saline aquifers: the influence of intra-aquifer shales and the relative effectiveness of structural, solubility and mineral trapping during prograde and retrograde sequestration. First Annual Conference on Carbon Sequestration. Geosciences and Environmental Division, Washington, D.C.

Joye, S.B., 2012. A piece of the methane puzzle. Nature 491, 538–539.

Kaszuba, J.P., Janecky, D.R., Snow, M.G., 2003. Carbon dioxide reaction processes in a model brine aquifer at 200 degrees C and 200 bars: implications for geologic sequestration of carbon. Appl. Geochem. 18 (7), 1065–1080.

Kaszuba, J.P., Janecky, D.R., Snow, M.G., 2005. Experimental evaluation of mixed fluid reactions between supercritical carbon dioxide and NaCl brine: relevance to the integrity of a geologic carbon repository. Chem. Geol. 217 (3–4), 277–293.

KØenen, M., Tambach, T.J., Neele, F.P., 2011. Geochemical effects of impurities in CO_2 on a sandstone reservoir. Energy Procedia 4, 5343–5349.

KØrbol, R., Kaddour, A., 1995. Sleipner-vest CO_2 disposal-injection of removed CO_2 into the Utsira formation. Energy Convers. Manag. 36 (6–9), 509–512.

Lasaga, A.C., 1984. Chemical-kinetics of water–rock interactions. J. Geophys. Res. 89 (Nb6), 4009–4025.

Lee, Y.-J., Morse, J.W., 1999. Calcite precipitation in synthetic veins: implications for the time and fluid volume necessary for vein filling. Chem. Geol. 156, 151–170.

Lindeberg, E., 2002. The quality of a CO_2 respository: what is the sufficient retention time of CO_2 stored underground. Proceedings of 6th International Conference on Greenhouse Gas Control Technologies, pp. 255–260.

Lindeberg, E., Wessel-Berg, D., 1997. Vertical convection in an aquifer column under a gas cap of CO_2. Energy Convers. Manag. 38 (Supplement(0)), S229–S234.

Lu, J., Wilkinson, M., Haszeldine, R.S., Fallick, A.E., 2009. Long-term performance of a mudrock seal in natural CO_2 storage. Geology 37 (1), 35–38.

Malik, Q.M., Islam, M.R., 2000. CO_2 injection in the Weyburn field of Canada: optimization of enhanced oil recovery and greenhouse gas storage with horizontal wells. Proceedings of the SPEDOE Improved Oil Recovery Symposium. SPE 59327, Tulsa, Oklahoma, USA, p. 16.

Moore, J., Adams, M., Allis, R., Lutz, S., Rauzi, S., 2005. Mineralogical and geochemical consequences of the long-term presence of CO_2 in natural reservoirs: an example from the Springerville-St. Johns Field, Arizona, and New Mexico, USA. Chem. Geol. 217 (3–4), 365–385.

Nagy, K.L., 1995. Dissolution and precipitation kinetics of sheet silicates. In: White, A.F., Brantley, S.L. (Eds.), Chemical Weathering Rates of Silicate Minerals. Mineralogical Society of America, 31. Washington, DC, pp. 173–233.

Parkhurst, D.L., Appelo, C.A.J., 1999. User's guide to PHREEQC (version 2) — a computer program for speciation, batch-reaction, one-dimensional transport and inverse geochemical calculations. U.S. Geological Survey Water Resources Investigations Report, pp. 99–4259.

Pokrovsky, O.S., Schott, J., 2001. Kinetics and mechanisms of dolomite dissolution in neutral to alkaline solutions revisited. Am. J. Sci. 301, 597–626.

Rimstidt, J.D., Barnes, H.L., 1981. The kinetics of silica–water reactions. Geochim. Cosmochim. Acta 44, 1683–1699.

Rochelle, C.A., Bateman, K., Pearse, J.M., 2002. Geochemical interactions between supercritical CO_2 and the Utsira Formation: an experimental study. British Geological Survey, Keyworth, Nottingham.

Rozalén, M.L., et al., 2008. Experimental study of the effect of pH on the kinetics of montmorillonite dissolution at 25 °C. Geochim. Cosmochim. Acta 72 (17), 4224–4253.

Rozalen, M., Huertas, F.J., Brady, P.V., 2009. Experimental study of the effect of pH and temperature on the kinetics of montmorillonite dissolution. Geochim. Cosmochim. Acta 73 (13), 3752–3766.

SACS2, 2002. Final technical report. EU Contract ENK6-CT-1999-00014.

Smith, J.W., Milton, C., 1966. Dawsonite in the Green River formation of Colorado. Econ. Geol. 61 (6), 1029–1042.

Stumm, W., Morgan, J.J., 1996. Aquatic Chemistry. Chemical Equilibria and Rates in Natural Waters. John Wiley and Sons (780 pp.).

Wiersma, C.L., Rimstidt, J.D., 1984. Rates of reaction of pyrite and marcasite with ferric iron at pH-2. Geochim. Cosmochim. Acta 48 (1), 85–92.

Wigand, M., Carey, J.W., Schutta, H., Spangenberg, E., Erzinger, J., 2008. Geochemical effects of CO_2 sequestration in sandstones under simulated in situ conditions of deep saline aquifers. Appl. Geochem. 23 (9), 2735–2745.

Worden, R.H., 2006. Dawsonite cement in the Triassic Lam Formation, Shabwa Basin, Yemen: a natural analogue for a potential mineral product of subsurface CO_2 storage for greenhouse gas reduction. Mar. Pet. Geol. 23 (1), 61–77.

Worden, R.H., Burley, S.D., 2009. Sandstone Diagenesis: The Evolution of Sand to Stone, Sandstone Diagenesis. Blackwell Publishing Ltd. 1–44.

Xu, T., Apps, J.A., Pruess, K., 2005. Mineral sequestration of carbon dioxide in a sandstone–shale system. Chem. Geol. 217 (3–4), 295–318.

Zerai, B., Saylor, B.Z., Matisoff, G., 2006. Computer simulation of CO_2 trapped through mineral precipitation in the Rose Run Sandstone, Ohio. Appl. Geochem. 21 (2), 223–240.